Passive vibration damping of hydrofoils using resonant piezoelectric shunt

Laetitia Pernod, Boris Lossouarn, Jacques-André Astolfi, Jean-François Deü

IX ECCOMAS Thematic Conference on Smart Structures and Materials
SMART 2019
A. Benjeddou, N. Mechbal and J.F. Deü (Eds)

PASSIVE VIBRATION DAMPING OF HYDROFOILS USING RESONANT PIEZOELECTRIC SHUNT

L. PERNOD[*†], B. LOSSOUARN[*], J.-A. ASTOLFI[†] AND J.-F. DEÜ[*]

[*] Laboratoire de Mécanique des Structures et des Systèmes Couplés (LMSSC),
Conservatoire national des arts et métiers (Cnam),
292 rue Saint-Martin, 75 003 Paris, France
email: laetitia.pernod@lecnam.net,
boris.lossouarn@lecnam.net
jean-francois.deu@cnam.fr,
www.lmssc.cnam.fr/en

[†] Institut de Recherche de l'Ecole Navale (IRENav)
EA 3634, Ecole Navale, 29 240, Brest, France
email: jacques-andré.astolfi@ecole-navale.fr,
www.ecole-navale.fr/en/The-Naval-Academy-Research%2C1804

Key words: Flow-induced vibrations, Resonant piezoelectric shunt, Passive vibration damping.

Abstract. Marine lifting surfaces undergo flow-induced vibrations leading to shorter life cycles due to structural fatigue and reduced acoustic performances. As such, accurate understanding of the fluid-structure response of marine structures, as well as vibrations control and damping, are critical to many maritime applications. In particular, this work investigates the potential of the electromechanical coupling inherent to piezoelectric materials for passive vibration damping of hydrofoils under hydrodynamic flows. An aluminium flat plate equipped with piezoelectric patches connected to a resonant shunt is considered. The structure is first tested under hydrodynamic flows for various Reynolds numbers to investigate its flow-induced vibrations. This allows to determine the natural frequency of interest to test the control solution. Second, an experimental modal analysis is carried out to determine the open and short circuit natural frequencies in order to compute the piezoelectric coupling factor. Indeed, the latter is related to the expected performance of the passive vibration damping strategy. Third, the values for the resistive and inductive components of the RL-shunt are inferred from the coupling factor and the natural frequencies. Last, the control solution is tested in still air and water in open and short circuits configurations. Comparisons of these two configurations are realised and the resonant shunt performance for vibration reduction of hydrofoils is estimated.

1 INTRODUCTION

Applications for high-speed ships fitted with hydrofoils, such as fast passenger-ferries and racing sailing boats, are progressively expanding and gaining economic importance. This leads to a renewed interest in the physical understanding of flow-induced vibrations of light flexible structures subjected to strong fluid-structure interactions. There is also a growing demand for vibration control and damping solutions. Indeed, flow-induced vibrations may trigger a sharp increase in the vibration amplitude when there is a coincidence between a natural frequency of the structure and a hydrodynamic excitation frequency. The consequences of such high-amplitude vibrations are reduced acoustic performances (*e.g.* hydrofoil singing), and shorter life cycles [1,2]. As such, it is of prime importance to develop methods for vibration damping.

Several researches have been completed on the high potential of piezoelectricity for vibration control and damping. In particular, Lossouarn et al. [3] and Thomas et al. in 2012 [4] in 2017 successfully demonstrated the ability of passive piezoelectric shunts to reduce the amplitude of the vibrations of structures in air. Academic research is now turning to the application of this solution to the maritime domain [5]. The purpose of this work is to provide a first experimental prototype for the application of vibration damping using a resonant piezoelectric shunt in water. The methodology used to assess the performance of the solution and design the electrical components of the resonant shunt (inductance and resonance) from the natural frequencies in open circuit and closed circuit is first described. We then present a case of application on a flat aluminium plate.

2 VIBRATION DAMPING USING A RESONANT PIEZOELECTRIC SHUNT

Vibration damping using piezoelectricity consists in converting part of the vibratory mechanical energy into electrical energy, which is then dissipated through a resistor R. Moreover, it is possible to create an electric resonance with the addition of an inductance L to the electrical circuit. When this electric resonance matches one of the natural frequencies of the structure the energy transfer is increased. As a consequence, a passive resonant piezoelectric shunt behaves similarly to a tuned mass-damper [3]. Figure 1 represents a model for a mass-spring system (mass m and stiffness K) coupled to a resonant piezoelectric shunt and subjected to a force F. U represents the displacement of the mass, q represents the electric charge displacement, C the capacitance of the piezoelectric patch, and e is the piezoelectric constant, R and L respectively being the resistance and the inductor of the shunt.

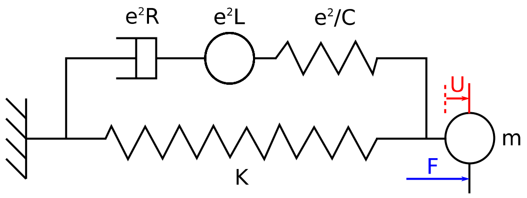

Figure 1: Purely mechanical model of a structure coupled to a resonant piezoelectric shunt

Important electrical conditions and their corresponding natural frequencies are the "short circuit" and "open circuit" conditions. The former corresponds to zero voltage across the piezoelectric patch and a natural frequency ω_{sc}, while the latter corresponds to zero electric charge displacement ($q = 0$) and to a natural frequency ω_{oc}. The performances of the vibration damping solution are only dependant on the coupling factor k_c defined by the short circuit and open circuit natural frequencies:

$$k_c = \sqrt{\frac{\omega_{oc}^2 - \omega_{sc}^2}{\omega_{sc}^2}} \tag{1}$$

Once the coupling factor is known, the electrical inductor and resistor of the resonant shunt have to be designed according to:

$$L = \frac{1}{C\omega_{oc}^2} \tag{2}$$

$$R = \sqrt{\frac{3}{2}}\,\frac{1}{C\omega_{oc}^2} \tag{3}$$

These conditions correspond to the optimal values of L and R in order to set the electrical resonance on the mechanical resonance of interest [5]. Passive inductors are then produced according to these specifications using copper wire and appropriate magnetic circuits.

3 EXPERIMENTAL SETUP AND TECHNIQUES

3.1 Experimental Facility and Sensors

Experiments were carried out in the hydrodynamic tunnel at the Institut de Recherche de l'Ecole Navale (IRENav) in Brest, France, illustrated on Figure 2. The tunnel test section is 1 m long with a 192 mm square section. Available operational velocities in the test section range from 0 m/s to 12 m/s and available pressures range from 0.1 bar to 3 bar. Both are set up using a regulation system. Moreover, a honeycomb grid upstream of the test section allows for a 2% free stream turbulent intensity at the mid-section. Vibration measurements are realised using a scanning Doppler laser vibrometer located above the structure and a single point Doppler laser vibrometer located below the structure. For more information about the hydrodynamic tunnel and the experimental techniques, the interested reader may refer to [1,6].

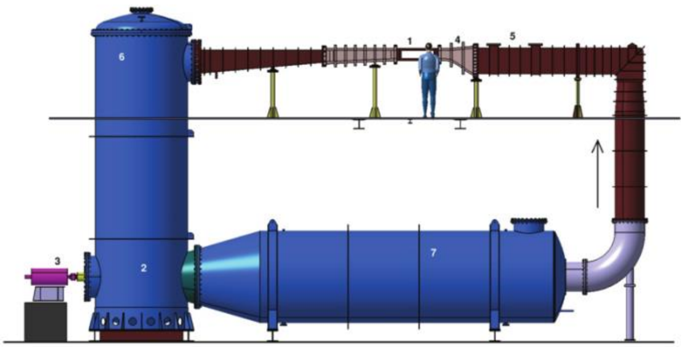

Figure 2: Hydrodynamic tunnel at IRENav, [6]

3.2 Geometry and Materials

The structure considered in this work is a flat plate made of aluminium 5083 and equipped with four piezoelectric patches (two patches on each side of the plate). Base dimensions of the plate are 191 mm x 100 mm x 6 mm, with a 80 mm x 31 mm x 10 mm extension at its base, as illustrated on Figure 3. This extension is used to clamp the structure to the tunnel wall. Furthermore, the piezoelectric patches are embedded in the structure *via* two pockets machined on both sides of the plate (Figure 3 and Figure 4). Indeed, embedding the patches in the structure avoids creating local roughness, which may cause added turbulence or flow detachment if the roughness size is in the order of the boundary layer thickness. The piezoelectric patches are vacuum-glued in the pockets using epoxy, then a layer of paraffin is added to fill the residual depth of the pocket. Pathways are also machined in the plate and the extension to allow the passage of cables from the electrodes (two on each patch) to the components of the electrical control circuit.

Figure 5 presents the geometry and dimensions of the piezoelectric transducers, in which a PIC 255 piezoelectric ceramic (black rectangle) is encapsulated. The dimensions of the patch are 61 mm long, 35 mm wide and 0.8 mm thick, for a piezoelectric part 50 mm long, 30 mm wide and 0.5 mm thick.

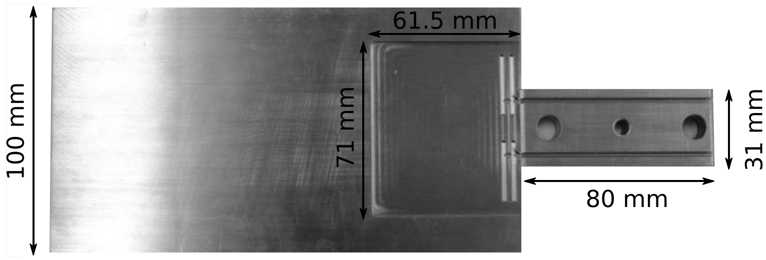

Figure 3: Geometry and dimensions of the structure

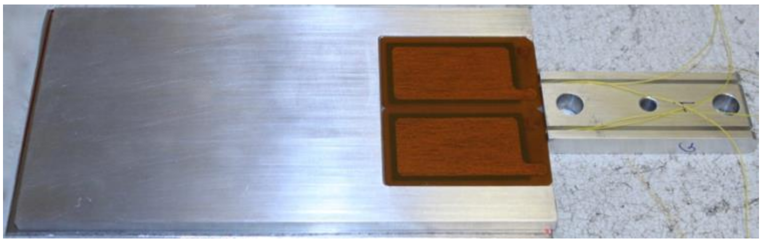

Figure 4: Flat plated equipped with the piezoelectric patches

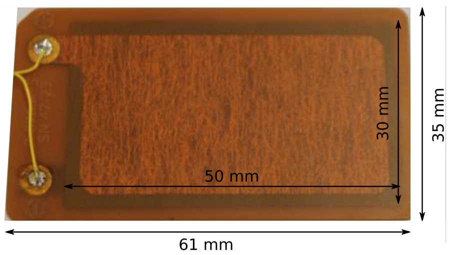

Figure 5: Geometry and dimensions of the piezoelectric patches

4 RESULTS

4.1 Test Cases Under Hydrodynamic Flows

Experiments are first carried out with the plate placed in water at an incidence of 0º, and incident flow velocities ranging from 1 m/s to 10.5 m/s, *i.e.* moderate Reynolds numbers from 10^5 to $1.05x10^6$. The objective is to investigate the flow-induced vibrations of the structure in order to determine the natural frequency of interest to test the control solution. Indeed, as detailed in Section 2, one has to know the value of the frequency to be controlled to guide the design choices of the electrical circuit (inductor and resistor). Therefore, piezoelectric patches are inactive in this first series of tests. Figure 6 shows the vibration spectra of the plate for the range of incident velocities considered. The first three natural frequencies are visible for respective values of 26.4 Hz, 174.1 Hz and 265.6 Hz. The spectra also exhibit additional components with a strong dependence to the Reynolds number: the local maximum close to 50 Hz for a Reynolds number of $1.5x10^5$ is progressively shifted towards the high frequencies when increasing the Reynolds number. This phenomenon is characteristic of a vortex shedding process associated to Von Kármán alleyways [1,2,7,8]: The boundary layer is developing on both sides of the plate but meets with a singularity at the trailing edge. The boundary layer then starts to shed alternatively from both sides of the plate, leading to the formation of a vortex street in the turbulent wake. This alternate shedding causes a periodic fluctuation of the hydrodynamic loads applied on the plate and is thus a source of excitation associated to a shedding frequency f_{shed}. In the present case, we can observe a strong fluid-structure interaction between the second mode of the structure (corresponding to the first torsion mode) and the shedding frequencies when their respective values coincide (around 174 Hz). This strong fluid-structure interaction is characterised by a sharp increase of the vibration amplitude.

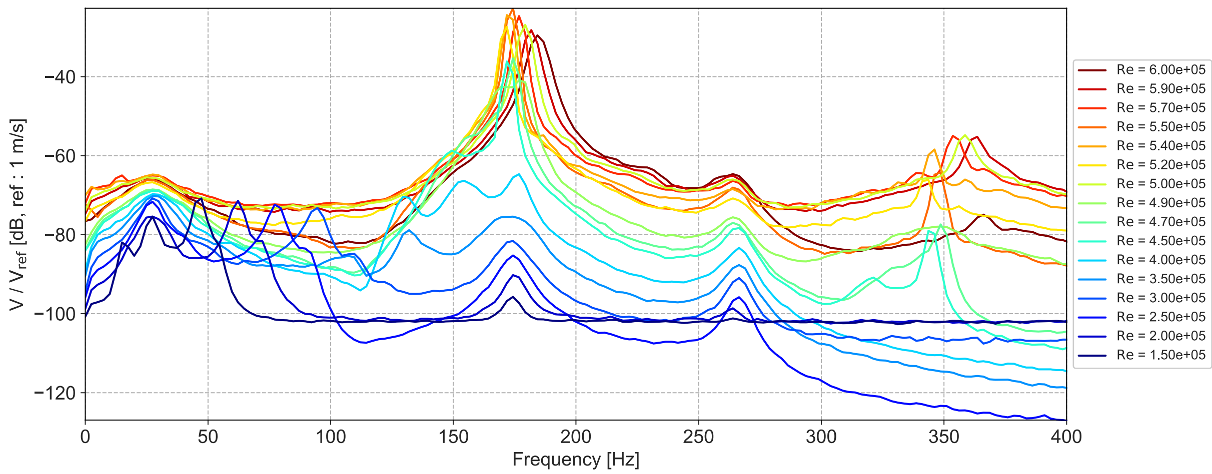

Figure 6: Vibration spectra under hydrodynamic flow for different incident velocities

Figure 7a presents the corresponding Reynolds-frequency diagram, which clearly highlights the linear evolution of the hydrodynamic excitation frequency with the Reynolds number, and therefore the velocity of the incident flow. This linear evolution is given by (4), with a constant Strouhal number close to 0.2 when vortex shedding occurs (*d* is the thickness of the plate and

U_0 the incident velocity) [7,8].

$$Sh = \frac{f_{shed} d}{U_0} \tag{4}$$

The linear evolution of the shedding frequencies with the Reynolds number according to Strouhal's law is also highlighted on Figure 7b, where the experimental data points correspond to the local maxima of the spectra presented on Figure 6. One can see that in the present case the Strouhal number is constant to 0.194, confirming the existence of vortex shedding. However, for some Reynolds numbers between $4x10^5$ and $6x10^5$ the shedding frequencies no longer follow Strouhal's law, but instead keep a constant value of 174 Hz, despite the increase in the number of Reynolds. This is the phenomenon of frequency lock-in around the first mode of torsion: Von Kármán's turbulent wake no longer evolves with its own dynamics (4) but is organized around the natural frequency of the structure [8,9]. As a consequence, the strong fluid-structure interaction previously mentioned corresponds to this lock-in phenomenon.

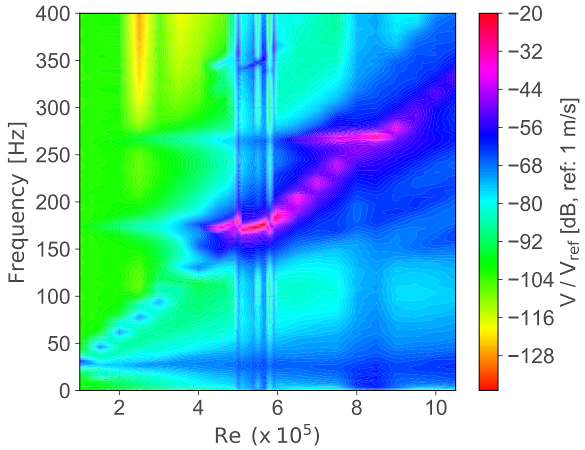

(a)

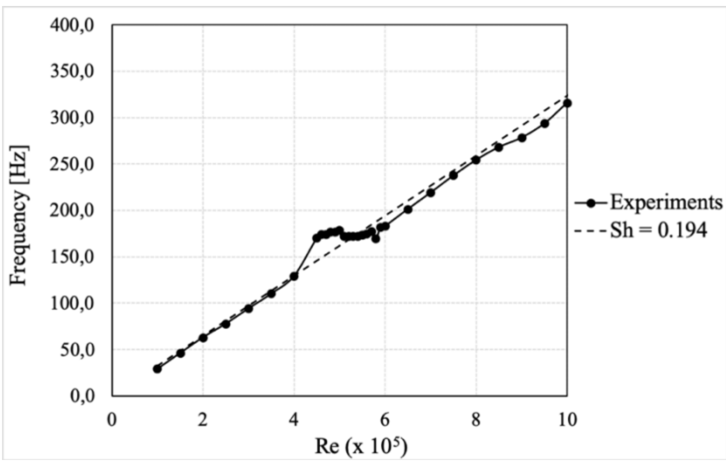

(b)

Figure 7: (a) Reynolds-frequency diagram and (b) shedding frequency vs Reynolds number and lock-in

4.2 Test Cases in Still Air and Water

The first series of tests highlighted the existence of a strong fluid-structure interaction between the first torsion mode and the hydrodynamic excitation frequencies due to Von Kármán vortex shedding, resulting in a large increase in the vibration amplitude. As a consequence, this structure is an interesting test case for the application of the vibration damping solution (described in Section 2) to the first torsion mode. The objective is to reduce the amplitude of the vibrations thanks to a passive resonant piezoelectric shunt adjusted on the natural frequency of the structure where the strong fluid-structure interaction occurs. As a first attempt for vibration damping in water using a piezoelectric shunt, this solution is indeed easier to setup than a Reynolds-dependent shunt that would follow the frequency shift of the hydrodynamic excitation.

For this purpose, a second series of tests is carried out both in air and then in still water in order to determine the open and short circuit natural frequencies and evaluate the performances of the control solution in a simplified case. Since the flow no longer provides the excitation of the structure, an alternative source of excitation is used: an electrical voltage is imposed on one of the patches (using a function generator) which then generates a vibratory excitation on the structure through the inverse piezoelectric effect. The other three patches are for the moment kept inactive. The main advantage of this method lies in its ability to provide the frequency responses functions (FRF) of the structure as both the input (voltage imposed on the patch) and output (velocity measured by the vibrometer) are known. On the contrary, when the excitation is generated by the hydrodynamic flow, the input is unknown. Here, a sinus excitation swept across the entire frequency band between 1 Hz and 100 Hz is applied on one of the patches. The temporal signal of this excitation is shown on Figure 8a and the corresponding temporal signal of the in-air and in-water responses are shown on Figure 8b.

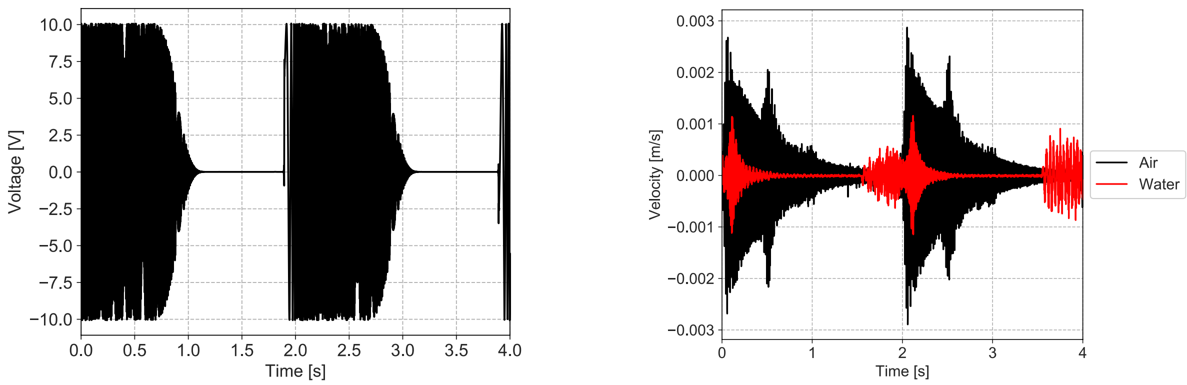

(a) (b)

Figure 8: Temporal signals associated to (a) the excitation by sweep and (b) the in-air and in-water vibrations of the structure

The frequency responses derived from the temporal signals are presented on Figure 9, where the first two modes of the structure are visible in air and the first three modes are visible in water. Corresponding values are reported in Table 1: the comparison of the natural frequencies in air and in water shows significant added mass effects, with a reduction of the in-air natural frequencies up to 58.8%.

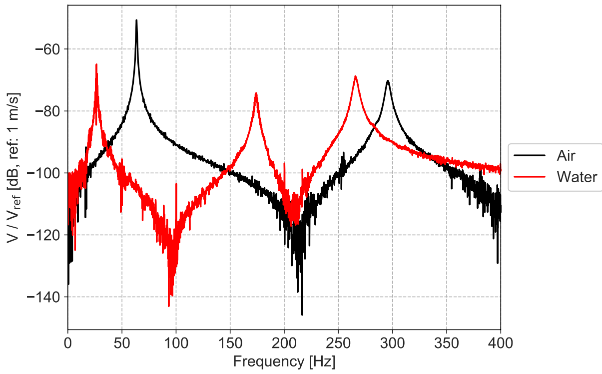

Figure 9: In-air and in-water frequency responses (without flow)

Table 1: Comparison of the in-air and in-water natural frequencies and added mass effects

	f_1	f_2	f_3
f_{air} [Hz]	63.3	295.9	-
f_{water} [Hz]	26.4	174.1	265.6
% f_{air}	58.3	41.2	-

Last, a third series of tests was performed to evaluate the performances of the coupling solution with one of the patches providing the excitation, and the other patches activated for vibration damping. However, the coupling factors obtained (of the order of 3% for the first torsion mode) did not allow to observe a significant reduction of the amplitude of vibration. Such low coupling factors may be explained, on the one hand, by a problem of water sealing on the cables, and on the other hand by a poor placement of the patches to control the first torsion mode. To tackle this issue, two solutions may be considered. First, smaller patches could be used. This way, the location of the patches would be better suited for the control of the first torsion mode. Another solution is to control the first bending mode instead of the first torsion mode, as the coupling factors are more favourable for the bending. However, in order to get an electrical signal that is strong enough for clear measurements, it is preferable to increase the frequency of the first bending mode, for instance by decreasing the length of the plate from 191 mm to 100 mm. This second solution is currently under investigation.

5 CONCLUSIONS

This work presents the testing in water of an aluminium flat plate equipped with four piezoelectric patches. It constitutes a first experimental assessment of vibration damping in water using a resonant piezoelectric shunt. The dynamic response of the structure under hydrodynamic flow was first studied for various incident velocities, then the performances of the control solution were estimated. Prior characterization of the dynamic response of the structure is indeed needed to determine the short and open circuit natural frequencies in order to compute the coupling factors and the optimal values for the inductance and resistance components of the piezoelectric shunt.

Results showed a strong fluid-structure interaction phenomenon between the natural frequencies of the structure and the hydrodynamic excitation frequencies due to Von Kármán vortex shedding in the turbulent wake. In particular, the hydrodynamic excitation frequencies present a linear dependence to the Reynolds number, with a constant Strouhal of 0.194, with the exception of a frequency lock-in around the first torsion mode (around 174 Hz). An original method for obtaining the frequency responses of the structure (FRF) in still water has also been implemented using one of the patches to provide the excitation of the structure, which allow non-contact excitation and measurement. However, the coupling factors obtained during these first tests to control the first torsion mode were too low to observe a significant reduction of the vibration amplitude, in particular due to a non-optimal placement of the piezoelectric patches. New tests are currently underway with a modified structure to ensure a better placement of the piezoelectric patches. A numerical analysis is also being carried out in order to numerically estimate the coupling factors before testing in water.

REFERENCES

[1] Lelong, A., Guiffant, P. and Astolfi, J.-A. An Experimental Analysis of the Structural Response of Flexible Lightweight Hydrofoils in Cavitating Flow. *J. Fluids Eng.* (2018) **2:**021116.

[2] Reese, M.C. Vibration and Damping of Hydrofoils in Uniform Flow. Ph.D. The Pennsylvania University (2010).

[3] Lossouarn, B., Aucejo, M., Deü J.-F. and Multon, B. Sensors and Actuators A: Physical Design of inductors with high inductance values for resonant piezoelectric damping *Sensors Actuators A. Phys.* (2017) **259**:68–76.

[4] Thomas, O., Ducarne, J. and Deü, J.-F. Performance of piezoelectric shunts for vibration reduction *Smart Mater. Struct.* (2012) **21**.

[5] Li, C., Chae, E.J., Young, Y.L., Wang, X. and Alben, S. Passive Vibration Control of Flexible Hydrofoils Using Piezoelectric Material. *Fourth International Symposium on Marine Propulsors*. (2015) Austin, Texas, USA.

[6] Gaugain, F. *Analyse expérimentale et simulations numériques de l'interaction fluide-structure d'un hydrofoil élastique en écoulements subcavitant et cavitant*, Ph.D. Ecole Nationale Supérieure d'Arts et Métiers (2013).

[7] Blake, W.K. Excitation of Plates and Hydrofoils by Trailing Edge Flows *J. Vib. Acoust. Stress. Reliab. Des.* (1984) **106**:351–63.

[8] Naudascher, E. and Rockwell, D. *Flow-Induced Vibrations: An Engineering Guide.* Dover Publications Inc. (2005).

[9] Zobeiri, A. *Effect of Hydrofoil Trailing Edge Geometry on the Wake Dynamics.* Ph.D. Ecole Polytechnique Fédérale de Lausanne (2012).